Neutron Star Matter EOS in RMF with Multi-Body Couplings

Akira Ohnishi[1], Kohsuke Tsubakihara[2,3], and Toru Harada[3]

[1] *Yukawa Institute for Theoretical Physics, Kyoto University, Kyoto 606-8502, Japan*
[2] *Academic Support Center, Kogakuin University, Nakano 2665-1, Hachioji, Tokyo 192-0015, Japan*
[3] *Department of Engineering Science, Faculty of Engineering, Osaka Electro-Communication University, Neyagawa 060-0810, Japan*

E-mail: ohnishi@yukawa.kyoto-u.ac.jp

(Received September 10, 2016)

We investigate the multi-body coupling effects on the neutron star matter equation of state (EOS). By tuning the multi-body coupling constants in the relativistic mean field (RMF) models, microscopic EOSs are well fitted, and smaller neutron star radii $R \sim 12$ km are obtained. When the repulsive potential for Λ at high density is assumed to have density dependence similar to that for nucleons, it is possible to support $2M_\odot$ neutron stars by hyperonic EOSs, which do not contradict hypernuclear data.

KEYWORDS: Hyperon puzzle, Three-baryon interaction, EOS, Relativistic mean field

1. Introduction

The hyperon puzzle is a serious problem in nuclear and hadron physics. Hypernuclear experiments show that the Λ potential in nuclei is attractive and the Pauli blocking does not operate on Λ in nuclear matter. Then the single particle energy of Λ at high densities can be smaller than the nucleon Fermi energy. Thus it is natural to expect that Λ would appear in neutron stars. Actually many model calculations suggest that Λ emerges in neutron star matter at baryon density $\rho_B \simeq (2-4)\rho_0$ with $\rho_0 \simeq 0.16\ \text{fm}^{-3}$ being the normal nuclear density. When hyperons appear in neutron star matter, the equation of state (EOS) is softened and the maximum mass of neutron stars is predicted to be $M_{\max} = (1.3-1.6)M_\odot$, which is significantly smaller than that without hyperons, $M_{\max} = (1.5-2.7)M_\odot$, where $M_\odot$ denotes the solar mass. The recent discovery of massive neutron stars, $M \sim 2M_\odot$ [1], then implies that most of the EOSs including hyperons are ruled out. We need to find the mechanisms to suppress hyperons at high densities or to stiffen the hyperonic matter EOS.

There are several mechanisms proposed so far to solve the hyperon puzzle [2,3]. Among the proposed mechanisms, 3B interactions [3] need to be included also in the nucleonic EOS. Microscopic (first principles) calculations have shown that 3B force is necessary to explain the binding energies of light nuclei [4] and nucleonic matter EOS [5–7]. The three-nucleon (3N) interaction has been discussed in chiral effective field theory (chiral EFT) [8], and chiral EFT based EOS has been obtained in microscopic calculations [9]. By comparison, 3B interactions including hyperons is not well determined. While hyperon-nucleon interactions are investigated in chiral EFT [10], we need much more accurate data on elementary processes in order to constrain the coefficients relevant to 3B interactions including hyperons in chiral EFT. In principle, lattice QCD can provide 3B interactions as demonstrated for the 3N interaction [11], but it seems that calculations of 3B interactions at physical quark masses require faster supercomputers and/or larger CPU time.

In the present proceedings, we try to combine the microscopic calculations of nucleonic matter and the hypernuclear phenomenology; We fit the relativistic mean field (RMF) parameters to the microscopic EOSs [5–7], and introduce Λ in a phenomenological manner with the potential depth of $U_\Lambda(\rho_0) = -30$ MeV. In order to take 3B interaction effects, we introduce multi-body coupling terms in RMF. We find that $2M_\odot$ neutron stars can be supported within the model uncertainties.

2. RMF with multi-body couplings and neutron star matter EOS

We consider the following RMF Lagrangian with multi-body couplings for nucleonic matter,

$$\mathcal{L} = \bar{\psi}(i\gamma^\mu\partial_\mu - M_N - U_s - \gamma^\mu U_\mu)\psi + \mathcal{L}_{\sigma\omega\rho}\ , \tag{1}$$

$$\mathcal{L}_{\sigma\omega\rho} = \frac{1}{2}\partial_\mu\sigma\partial^\mu\sigma - \frac{1}{4}\omega_{\mu\nu}\omega^{\mu\nu} - \frac{1}{4}\boldsymbol{R}_{\mu\nu}\cdot\boldsymbol{R}^{\mu\nu} - \mathcal{V}_{\sigma\omega\rho}\ , \tag{2}$$

$$U_s = -g_\sigma\sigma\left[1 + r_{\sigma\sigma}(1-\sigma/f_\pi)\right] + g_\sigma\omega^\mu\omega_\mu\left[r_{\omega\omega} + r_{\sigma\omega\omega}(1-\sigma/f_\pi)\right]\ , \tag{3}$$

$$U_\mu = g_\omega\omega_\mu\left[1 - r_{\sigma\omega}\sigma/f_\pi + r_{\omega3}\omega^\nu\omega_\nu/f_\pi^2\right] + g_\rho\boldsymbol{\tau}\cdot\boldsymbol{R}_\mu\left[1 - r_{\sigma\rho}\sigma/f_\pi + r_{\omega\rho}\omega^\nu\omega_\nu/f_\pi^2\right]\ , \tag{4}$$

$$\begin{aligned}\mathcal{V}_{\sigma\omega\rho} =& \frac{1}{2}m_\sigma^2\sigma^2 - a_\sigma f_{\log}(\sigma/f_\pi) + \frac{1}{4}c_{\sigma4}(\sigma^4 - 4f_\pi\sigma^3) - \frac{1}{2}m_\omega^2\omega^\mu\omega_\mu\left[1 - c_{\sigma\omega}\sigma/f_\pi\right] - \frac{1}{4}c_{\omega4}(\omega^\mu\omega_\mu)^2 \\ & - \frac{1}{2}m_\rho^2\boldsymbol{R}^\mu\cdot\boldsymbol{R}_\mu\left[1 - c_{\sigma\rho}\sigma/f_\pi + c_{\omega\rho}\omega^\mu\omega_\mu/f_\pi^2\right] - \frac{1}{4}c_{\rho4}(\boldsymbol{R}^\mu\cdot\boldsymbol{R}_\mu)^2\ ,\end{aligned} \tag{5}$$

where $\omega_{\mu\nu}$ and $\boldsymbol{R}_{\mu\nu}$ denote the field tensors of ω and ρ mesons, respectively, and $f_{\log}(x) = \log(1-x) + x + x^2/2$ [12]. This Lagrangian contains $n = 3$ and $n = 4$ terms where $n = B/2 + M$ with B and M being the number of baryon fields and non-NG bonson fields, respectively [13]. Terms with the index n generate n-body interactions. By tuning the coefficients, we fit microscopic (first principles) EOSs, FP [5], DBHF [6] and APR [7]. Similar analysis was performed in Ref. [14] for APR. We apply a stochastic method to determine parameters, resulting in the standard deviation of $(0.5 - 1.0)$ MeV in the energy per nucleon. In Fig. 1, we show EOSs (left), the symmetry energy (middle), and the neutron star matter EOSs (right). As shown in the left panel of Fig. 2, suppressed pressure at low density compared with standard RMF models leads to smaller neutron star radii, $R \simeq 12$ km, which is consistent with the X-ray burst analysis [15].

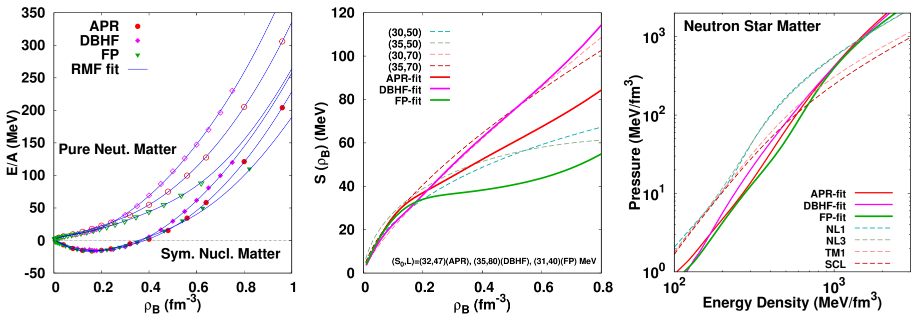

Fig. 1. EOS of symmetric nuclear matter and pure neutron matter (left), symmetry energy as a function of baryon density (middle), and neutron star matter EOS (right).

We introduce Λ hyperons in two schemes; In Scheme 1, we assume that the potential for Λ is proportional to that for N, $U_\Lambda = \alpha\, U_N$, where the potential is given as the sum of the scalar potential and the temporal component of the vector potential. In Scheme 2, we assume that the potential for Λ is given as $U_\Lambda = 2/3U_N^{(n=2)} + \beta\, U_N^{(n\geq3)}$, where the superscripts show $n = 2$ and $n = 3$ parts of U_N. Coefficients α and β are determined to reproduce $U_\Lambda(\rho_0) = -30$ MeV. In the right panel of Fig. 2, we show the single particle energy of Λ at zero momentum, $E_\Lambda(p = 0) = M_\Lambda + U_\Lambda$, as a function of density. We find that Scheme 1 gives more repulsive U_Λ at high densities, and the maximum mass of neutron stars in Scheme 1 becomes around $2M_\odot$.

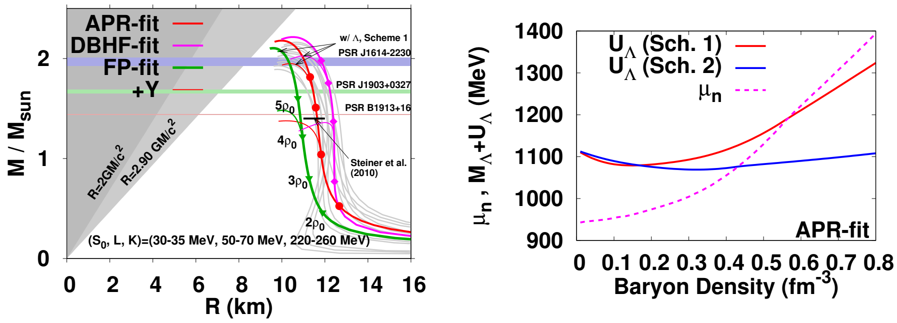

Fig. 2. Mass-radius relation of neutron stars (left) and Λ potential in nuclear matter (right).

3. Summary

We have investigated the role of multi-body couplings in the equation of state (EOS) of nuclear and neutron star matter. In the relativistic mean field (RMF) models with multi-body coupling terms, we can reproduce the suppression of the symmetry energy at high densities found in microscopic EOSs [5–7]. As a result, smaller neutron star radii $R \sim 12$ km are obtained. We have also found that hyperonic EOSs constrained by the hypernuclear physics requirement $U_\Lambda(\rho_0) \simeq -30$ MeV can support $2M_\odot$ neutron stars when the repulsive potential for Λ at high density has density dependence similar to that for nucleons. This density dependence should be examined by studying the separation energy of Λ in various finite hypernuclei.

This work is supported in part by the Grants-in-Aid from JSPS (Nos. 15K05079, 15H03663, and 16K05350), and by the Grants-in-Aid from MEXT (Nos. 24105001, 24105008).

References

[1] P. Demorest *et al.*: Nature **467** (2010) 1081; J. Antoniadis *et al.*: Science **340** (2013) 6131.
[2] S. Weissenborn *et al.*: Nucl. Phys. A **881** (2012) 62; I. Bednarek *et al.*: Astron. Astrophys. **543** (2012) A157; T. Miyatsu *et al.*: ApJ **777** (2013) 4; W. Z. Jiang *et al.*: ApJ **756** (2012) 56; W. H. Long *et al.*: Phys. Rev. C **85** (2012) 025806; K. A. Maslov *et al.*: Phys. Lett. B **748** (2015) 369; L. Bonanno, A. Sedrakian: Astron. Astrophys. **539** (2012) A16; K. Masuda *et al.*: ApJ **764** (2013) 12; PTEP **2013** (2013) 073D01.
[3] Y. Yamamoto *et al.*: Phys. Rev. C **90** (2014) 045805; D. Lonardoni *et al.*: Phys. Rev. Lett. **114** (2015) 092301; K. Tsubakihara and A. Ohnishi: Nucl. Phys. A **914** (2013) 438.
[4] J. Carlson *et al.*: Rev. Mod. Phys. **87** (2015) 1067.
[5] B. Friedman and V. R. Pandharipande: Nucl. Phys. A **361** (1981) 502.
[6] G. Q. Li, R. Machleidt and R. Brockmann: Phys. Rev. C **45** (1992) 2782.
[7] A. Akmal, V. R. Pandharipande and D. G. Ravenhall: Phys. Rev. C **58** (1998) 1804.
[8] R. Machleidt and D. R. Entem, Phys. Rept. **503** (2011) 1.
[9] M. Kohno, Phys. Rev. C **88** (2013) 064005.
[10] J. Haidenbauer *et al.*: Nucl. Phys. A **915** (2013) 24.
[11] T. Doi *et al.* [HAL QCD Collaboration], Prog. Theor. Phys. **127** (2012) 723.
[12] K. Tsubakihara and A. Ohnishi: Prog. Theor. Phys. **117** (2007) 903.
[13] R. J. Furnstahl, B. D. Serot and H. B. Tang: Nucl. Phys. A **615** (1997) 441 [Errata; 640 (1998), 505].
[14] A. W. Steiner *et al.*: Phys. Rept. **411** (2005) 325; A. W. Steiner *et al.*: ApJ **774** (2013) 17.
[15] A. W. Steiner, J. M. Lattimer and E. F. Brown: Astrophys. J. **722** (2010) 33.